Electric Field Controlled, Pulsed Autoionization in Two Electron Wave Packets

J. G. Story and Heider N. Ereifej
Department of Physics, University of Missouri–Rolla, Rolla, Missouri 65409-0640
(Received 5 July 2000)

In this paper, control of the evolution of a two electron wave packet through the application of a static electric field is demonstrated. Specifically, application of a small electric field is used to produce pulsed autoionization events, the timing of which can be controlled on a picosecond time scale. The technique is demonstrated by exciting calcium atoms using a short-pulsed laser to the $4p_{3/2}19d$ doubly excited state, which is energy degenerate with the $4p_{1/2}nk$ stark states. Evolution of the resultant wave packet is monitored through the application of a second short laser pulse, which stimulates the atoms to emit a photon producing singly excited Rydberg states which are detected using field ionization.

DOI: 10.1103/PhysRevLett.86.612 PACS numbers: 32.80.Rm, 33.80.Rv

Rydberg electron wave packet evolution has been the subject of considerable interest in recent years. This interest stems from both a fundamental interest in the bridge between quantum and classical systems and, second, because Rydberg wave packets provide an excellent system in which to study control of the evolution of quantum systems [1,2]. In addition to evolution in the radial direction [3], it is possible to generate angular evolution of electronic wave packets by exciting atoms using a short-pulsed laser in the presence of a static electric field [4–8]. The static field causes an energy splitting of the angular momentum manifolds of atoms, producing Stark states in which the energy spacing between states depends on the size of the applied field [9]. The evolution of wave packets is highly dependent on the spacing between states, making Stark states an excellent system in which to study temporal dynamics, since the evolution of the wave packets can be controlled by simply changing the size of the applied electric field. The use of Rydberg wave packets in the study of doubly excited atoms has been shown to be a useful tool for studying the dynamical interaction between the two excited electrons [10–20]. The use of applied electric fields to control the evolution of the two electron wave packets provides a sensitive tool in the study of the interelectron interaction.

Of particular interest are doubly excited states above the first ionization limit where autoionization can occur. It has recently been shown that autoionization occurs in a steplike fashion, when atoms are excited using short-pulsed lasers [21–24]. The stepwise decay arises from the periodic orbit of the Rydberg electron in a wave packet state. In the following we show that, by applying small static electric fields to atoms under the proper conditions, the timing between autoionizing events can be accurately controlled. This ability to control the decay of the atoms produces bursts of electrons on a picosecond time scale, with the timing determined by the applied electric field. A critical element in the control of the autoionization process is shown to be the coupling between two doubly excited electron configurations, one which autoionizes rapidly and one which has an extremely long lifetime. Oscillation between these two configurations produces the pulsed autoionization effect, with the rate of oscillation controllable through the application of a small electric field. It has been demonstrated that the presence of a static electric field can increase the cross section for dielectronic recombination [25–27], a process by which an electron is captured by an ion into a doubly excited state, which is then stabilized through photoemission. The present experiment will show the dynamics of electric field enhancement of the recombination process.

As shown in Fig. 1, two dye lasers producing 3 ns pulses were used to promote calcium from the ground state to the $4s19d$ Rydberg state. 50 ns later the atoms were exposed to a 393.5 nm, 500 fs laser pulse tuned to the $4s19d$-$4p_{3/2}19d$ transition. In the absence of a static field, the $4p_{3/2}19d$ state is energy degenerate with the $4p_{1/2}nl$ doubly excited states, with n centered around 31, and with several continua channels. The $4p_{3/2}19d$ state is strongly coupled to the $4p_{1/2}nd$ states. Excitation with the short laser pulse produced a nearly pure $4p_{3/2}19d$ state, since the excitation time was shorter than the autoionization lifetime of this state. As a result, a nonstationary two-electron wave packet was produced which could then evolve into the degenerate bound and continuum dielectronic configurations. Evolution into the $4p_{1/2}nl$ channel was monitored using a second 397 nm, 500 fs laser pulse, tuned to stimulate the atoms to make a core transition from the $4p_{1/2}nl$ doubly excited state to the $4snl$ singly excited neutral configuration. The resulting $4snl$ states had lifetimes of several μs, allowing selective field ionization detection of these states to be performed. A direct and complete monitoring of the evolution of these autoionizing states was made possible by simply changing the timing between the first and second short pulsed lasers. If a small static electric field was applied to the atoms, the $4p_{3/2}19d$ state was relatively unaffected, whereas the $4p_{1/2}nl$ states, due to the higher n values, became $4p_{1/2}nk$ Stark states through mixing of angular momenta. The experiment consisted of monitoring the final field ionization signal while scanning the timing between the two short laser pulses for a number of different values of applied electric field.

 0031-9007/01/86(4)/612(4)$15.00

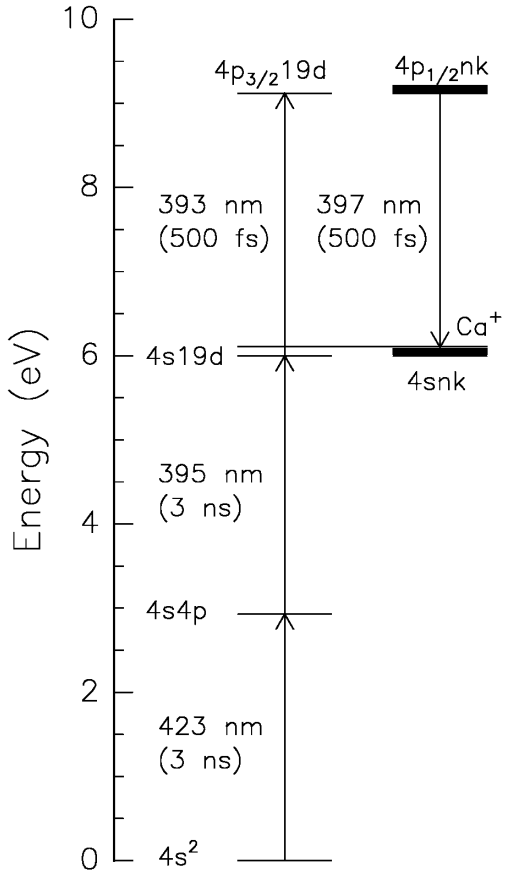

FIG. 1. Excitation diagram for calcium used in the experiment. The first two nanosecond dye lasers excite the $4s^2\,{}^1S_0$ ground state to a high Rydberg level ($4s19d\,{}^1D_2$). 50 ns later a 500 fs laser pulse promotes the atom to a pure $4p_{3/2}19d$ doubly excited state. A second 500 fs pulse with a variable temporal delay is then used to drive the transition from the $4p_{1/2}nk$ doubly excited Stark state to the $4snk$ state, which can be detected by field ionization.

The short laser pulses used in this experiment were produced using an amplified self-mode-locked Ti:sapphire laser. The system produced 4 mJ, 100 fs laser pulses with a repetition rate of 20 Hz. The full width at half maximum (FWHM) of the pulses was 160 cm^{-1}, with central wavelength at 790 nm. With this spectral width, it was possible to produce wavelengths resonant with the transition from the $4s$ ground ionic state of calcium to both $4p$ fine structure states from a single laser, simply by splitting the beam into two parts and using two separate 1.2 cm KDP (potassium dihydrogen phosphate) doubling crystals, each tuned to the proper wavelength. By doing so, nearly zero temporal jitter between the two short pulses was achieved. A variable optical path length allowed continuous scanning of the delay between the two laser pulses. The KDP doubling crystals limited the pulse bandwidth to about 30 cm^{-1}, which corresponds to approximately 500 fs laser pulse duration. It should be noted that the frequency doubling process can have the effect of temporally broadening the laser pulse, creating a pulse which is not transform limited. These effects were sufficiently small in this experiment that they had a negligible effect on experimental results. The experiment was performed in a vacuum chamber with background pressures in the low 10^{-7} Torr. The lasers were focused and crossed in the interaction region, where they interacted with a calcium atomic beam at a right angle. The atomic beam was produced by a resistively heated effusive stainless steel oven that produced an atomic density of about 10^{10} atoms/cm^3. Capacitor plates were placed above and below the interaction region with a screen mesh in the top capacitor plate allowing electrons to pass. Above the interaction region a microchannel-plate charged particle detector was used to monitor electrons produced in the experiment. Detection of the final $4snk$ Stark electron population was accomplished using a ramped negative voltage applied to the lower capacitor plate, which produced a time resolved field ionization signal consisting of all atoms which made the $4p_{1/2}nk$ to $4snk$ transition.

The detailed theory of the oscillation between bound two-electron channels is given elsewhere [24] and will be briefly outlined here. The true energy eigenstates at the energy of the $4p_{3/2}19d$ state are a combination of $4p_{3/2}19d$, $4p_{1/2}nl$, and continuum character. At any given energy, multichannel quantum defect theory can be used to calculate the amount of character from each of the electronic configurations [28]. For an atom initially prepared in the $4s19d$ state, which is excited by a laser tuned to the $4s$ to $4p_{3/2}$ ion transition, the excitation cross section is dominated by the $4p_{3/2}19d$ character [29]. If the excitation laser has a sufficiently short pulse, then a wave packet will be produced which consists solely of $4p_{3/2}19d$ character at the time of creation. This is possible because the wave packet consists of a range of energy eigenstates with relative phases such that the $4p_{3/2}19d$ character adds constructively and the $4p_{1/2}nl$ and continuum character add destructively [24]. An alternate way of viewing this process is simply that the core electron is excited on a time scale insufficient for the Rydberg electron to react to the change in the core. As the wave packet evolves, continuum character will develop which is the autoionization process. Also, $4p_{1/2}nl$ character will develop as a wave packet of n states centered around $n = 31$ with primarily $l = d$ since the $4p_{3/2}19d$ state is coupled mainly to the $4p_{1/2}nd$ channel. As time progresses an oscillation between the two bound channels occurs which is accompanied by autoionization [24]. The oscillation period of the wave packet is determined by the spacing between the $4p_{1/2}nd$ states:

$$T = 2\pi n^3 \tag{1}$$

in a.u., where n is the central quantum number of the wave packet and the spacing between states is n^{-3}.

In the presence of a small electric field the $4p_{3/2}19d$ state is relatively unaffected due to the low value of n for the Rydberg electron. However, the $4p_{1/2}nl$ states are mixed into Stark states. As with zero-field excitation, the initial wave packet is a nearly pure $4p_{3/2}19d$ state, which

is now coupled to the $4p_{1/2}nk$ Stark states. Time evolution of the wave packet will produce a Stark wave packet which will initially have mainly d angular momentum. As time continues, the Stark wave packet will develop higher angular momentum which will effectively decouple the $4p_{1/2}nk$ states from the initial $4p_{3/2}19d$ state, since the high angular momentum Rydberg electron has very little overlap with the core electron. This decoupling produces a time period in which virtually no autoionization can occur. Eventually the Stark wave packet returns to its initial condition, in a time period determined by the energy spacing between Stark states, which is in turn controlled by the strength of the external electric field. At this time, autoionization can occur producing a pulse of electrons. Those atoms which survive will undergo a second oscillation of the Stark wave packet. The energy spacing between states is given by

$$\Delta E = \alpha F, \tag{2}$$

where α is a measure of the linear polarizability which depends on the particular atom and on n, and F is the electric field strength. The oscillation period is thus given by

$$T = 2\pi(\alpha F)^{-1}. \tag{3}$$

Figure 2 shows data for a range of applied electric fields. For zero field the population in the doubly excited states autoionizes rapidly as seen in Fig. 2(a). This process occurs in a stepwise manor, which can be seen in the figure, due to radial oscillation of the Rydberg wave packet [24]. The small residual tail seen in this figure is most likely due to small stray fields in the interaction region. With a small applied field, shown in Fig. 2(b), a significant amount of population survives the initial autoionization event (autoionization events are characterized by a rapid decrease in population). This residual population shows no sign of further autoionization until approximately 300 ps later, at which time a second rapid autoionization event occurs. This autoionization event produces a pulse of electrons approximately 300 ps after the initial pulse. As the applied electric field is increased, the oscillation period is reduced as expected, so that the second autoionization comes earlier in time, as seen in Figs. 2(c) and 2(d). For sufficiently large applied field, the $n = 19$ state is significantly Stark split and the Stark manifolds of adjacent n states around $n = 31$ begin to overlap. This produces a much more complicated spectra and the simple oscillation pattern is no longer observed, as can be seen in Fig. 2(e). The decay of the doubly excited states appears to become more nearly exponential for the case of a strong applied field. The transition between pulsed decay and exponential decay for increasing field is not considered here, but would provide an interesting subject for further study.

The amount of population that survives the initial autoionization event increases with increasing applied field. This increase is due to a more rapid decoupling of the two electrons at the increased oscillation frequency. For small applied fields, as seen in Fig. 2(b), very little high angular momentum character has developed in the wave packet before the return to the $4p_{3/2}19d$ state. As the oscillation rate increases the high angular momentum character develops more rapidly so that decoupling of the electrons occurs before the return to the $4p_{3/2}19d$ state. Figure 2(d) shows that for sufficiently rapid oscillation rates a significant amount of population survives the second autoionization event producing further oscillations. Since the $4p_{1/2}nd$ states in calcium are the most rapidly autoionizing states of the $4p_{1/2}nl$ angular momentum states, we can estimate the survival rate using the autoionization lifetime and the dephasing time of the Stark wave packet, which will eliminate the d character through destructive interference. The autoionization lifetime can be obtained directly from Fig. 2(a) which gives $\tau_{\mathrm{AI}} = 13 \pm 2$ ps. The dephasing time t_d, if we assume equal d character in all Stark states, is inversely proportional to the energy width of the Stark manifold which gives a dephasing time of $1/30$ the Stark oscillation period. However, the d character is not equally distributed in the Stark states [9], which increases the dephasing time by a factor of approximately 2. Using this approximation the percentage of population which survives

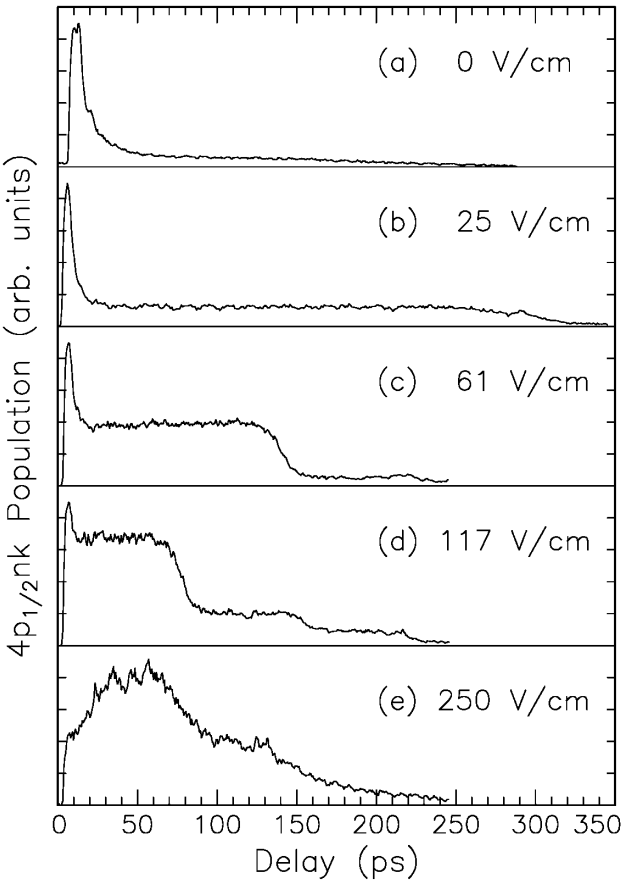

FIG. 2. The $4p_{1/2}nk$ population versus delay between the two short laser pulses is shown for a range of applied electric fields. The signal is obtained from field ionization of the $4snk$ states resulting from stimulated emission out of the $4p_{1/2}nk$ states. Periods of rapid population decrease represent autoionization events.

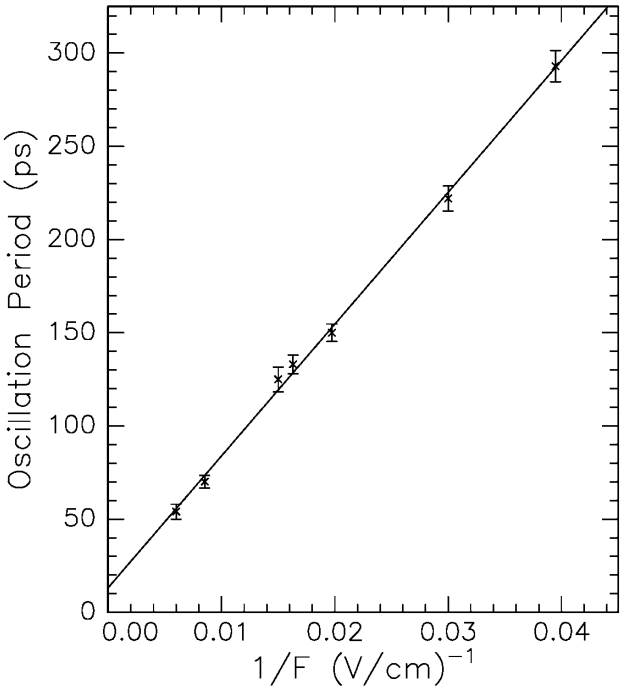

FIG. 3. The wave packet oscillation period versus the inverse of the applied electric field F is shown along with a linear fit to the data. The error bars represent the full width at half maximum of the autoionization pulses.

the first autoionization event can be calculated using an exponential decay model $\exp(-t_d/\tau_{\mathrm{AI}})$ to be 21%, 49%, and 70% for electric field strengths of 25, 61, and 117 V/cm, which is in reasonable agreement with the data in Fig. 2.

The data clearly demonstrate the effect of electric fields on dielectronic recombination, if we treat the $4p_{3/2}19d$ state as a continuum of finite bandwidth [26,27]. For a sufficiently small electric field, the wave packet simply makes one radial oscillation and the majority of the population returns to the continuum. For higher electric fields the electrons decouple due to the evolution of high angular momentum components, thereby increasing the amount of time available for photoemission.

Figure 3 shows the oscillation period versus the inverse of the electric field. It should be noted that the fit does not intersect zero oscillation period. The slight discrepancy is the result of the additional radial oscillation of the wave packet. The fit to the data gives a value of the polarizability $\alpha = 110 \pm 5$ a.u. which is reasonably close to the hydrogenic value $\alpha = 3n = 93$ a.u. [9].

The coupling between the two bound electronic configurations plays an important role in our ability to control the timing of the pulsed autoionization, by allowing us to produce a wave packet which is initially composed of low angular momentum character. The long periods of stability of the doubly excited population clearly demonstrate the decoupling effects of the evolution of the Stark wave packets, and the relatively short autoionization events show the return to low angular moment character.

The authors would like to thank Robert R. Jones and Paul E. Parris for numerous helpful and interesting discussions. This work was supported by the National Science Foundation (Grant No. 9722561) and the University of Missouri Research Board.

[1] T. C. Weinacht, J. Ahn, and P. H. Bucksbaum, Phys. Rev. Lett. **80**, 5508 (1998).
[2] T. C. Weinacht, J. Ahn, and P. H. Bucksbaum, Phys. Rev. Lett. **81**, 3050 (1998).
[3] A. ten Wolde *et al.,* Phys. Rev. Lett. **61**, 2099 (1988).
[4] L. D. Noordam *et al.,* Phys. Rev. A **40**, 6999 (1989).
[5] G. M. Lankhuijzen and L. D. Noordam, Phys. Rev. A **52**, 2016 (1995).
[6] G. M. Lankhuijzen and L. D. Noordam, Phys. Rev. Lett. **76**, 1784 (1996).
[7] V. G. Stavros and H. H. Fielding, Chem. Phys. Lett. **284**, 93 (1998).
[8] B. S. Mecking and P. Lambropoulos, Phys. Rev. Lett. **83**, 1743 (1999).
[9] T. F. Gallagher, *Rydberg Atoms* (Cambridge University Press, Cambridge, England, 1994), 1st ed.
[10] J. G. Story, D. I. Duncan, and T. F. Gallagher, Phys. Rev. Lett. **71**, 3431 (1993).
[11] D. W. Schumacher, D. I. Duncan, R. R. Jones, and T. F. Gallagher, J. Phys. B **29**, L1 (1996).
[12] D. W. Schumacher, B. J. Lyons, and T. F. Gallagher, Phys. Rev. Lett. **78**, 4359 (1997).
[13] B. J. Lyons *et al.,* Phys. Rev. A **57**, 3712 (1998).
[14] M. B. Campbell, T. J. Bensky, and R. R. Jones, Phys. Rev. A **57**, 4616 (1998).
[15] B. S. Mecking and P. Lambropoulos, Phys. Rev. A **57**, 2014 (1998).
[16] X. Chen and J. A. Yeazell, Phys. Rev. A **58**, 1267 (1998).
[17] B. S. Mecking and P. Lambropoulos, J. Phys. B **31**, 3353 (1998).
[18] X. Chen and J. A. Yeazell, Phys. Rev. Lett. **81**, 5772 (1998).
[19] R. van Leeuwen, M. L. Bajema, and R. R. Jones, Phys. Rev. Lett. **82**, 2852 (1999).
[20] X. Chen and J. A. Yeazell, Phys. Rev. A **60**, R4229 (1999).
[21] X. Wang and W. E. Cooke, Phys. Rev. Lett. **67**, 976 (1991).
[22] J. E. Thoma and R. R. Jones, Phys. Rev. Lett. **83**, 516 (1999).
[23] J. B. M. Warntjes, C. Wesdorp, F. Robicheaux, and L. D. Noordam, Phys. Rev. Lett. **83**, 512 (1999).
[24] H. N. Ereifej and J. G. Story, Phys. Rev. A **62**, 33 405 (2000).
[25] A. Muller *et al.,* Phys. Rev. A **36**, 599 (1987).
[26] J. G. Story, B. J. Lyons, and T. F. Gallagher, Phys. Rev. A **51**, 2156 (1995).
[27] L. Ko, V. Klimenko, and T. F. Gallagher, Phys. Rev. A **59**, 2126 (1999).
[28] W. E. Cooke and C. L. Cromer, Phys. Rev. A **32**, 2725 (1985).
[29] W. E. Cooke, T. F. Gallagher, S. A. Edelstein, and R. M. Hill, Phys. Rev. Lett. **40**, 178 (1978).